

ABSOLUTE CROSS SECTION FOR THE PRODUCTION
OF ^{24}Na IN Cu BY 400-GeV PROTONS

S. I. Baker, C. R. Kerns, and S. d. Pordes
Fermi National Accelerator Laboratory
Batavia, Illinois 60510, U.S.A.

J. B. Cumming and A. Soukas
Brookhaven National Laboratory
Upton, New York 11973, U.S.A.

V. Agoritsas and G. R. Stevenson
CERN, European Organization for Nuclear Research
1211 Geneva 23, Switzerland

Abstract

The absolute cross section for the production of ^{24}Na in natural Cu by 400-GeV protons has been determined to be (3.90 ± 0.11) mb. The quoted error includes both statistical and systematic uncertainties. In this work intensities of the Fermilab one-millisecond spill proton beam were measured using two independent beam current transformer systems which were calibrated electrically in situ. The ^{24}Na produced in the Cu foils was assayed by comparing the intensity of its 1368-keV γ ray with that of the 1332-keV γ ray from ^{60}Co standards.

Submitted to Nuclear Instruments and Methods
November 2, 1983

1. Introduction

Foil activation techniques have come to play an important supplementary role in beam measurement and diagnosis at high-energy accelerators. Although beam intensities can be measured most conveniently for routine applications by on-line devices such as beam current transformers or secondary emission chambers (SEC's) which can be read on a pulse-by-pulse basis, such devices have some limitations. For example, although beam current transformers can be calibrated absolutely by passing well-measured currents through them, they are limited by the signal-to-noise ratio to use in high-intensity, fast spill beams (milliseconds or less). A SEC can be used for either a fast or a slow spill (seconds or more in duration). However, its response depends on the surface treatment of the foils and their previous irradiation history. Stability over a wide range of operating conditions can be achieved,¹ but it cannot be calibrated absolutely and directly.

Foil activation is linear over a very wide intensity range and is insensitive to the temporal structure of a beam pulse. Thus, foil activation can be used in slow spill beams to calibrate secondary emission chambers and ion chambers in situ, once the activation cross section has been measured. The present paper describes measurements of the cross section for forming ^{24}Na from natural Cu by irradiation with 400-GeV protons at the Fermi National Accelerator Laboratory (Fermilab). In this work beam intensities were determined by two beam current transformers.^{2,3}

Choice of this particular activation reaction has several advantages:

(1) The high effective threshold (cross section ~ 0.05 mb at 0.4 GeV^4 compared to a peak value of ~ 4 mb) makes the result less sensitive to low-energy hadrons and, thus, less dependent on beam quality than ^{24}Na production in Al or ^{11}C production in carbon.⁵

(2) Detection of γ rays from ^{24}Na avoids sample thickness problems associated with the detection of alpha particles from ^{149}Tb in Au foils, another high-threshold monitor reaction which has been used in the past.⁶

(3) The convenient availability of calibrated standards of ^{60}Co which has a γ ray at 1332 keV, in close proximity to the ^{24}Na γ ray at 1368 keV, provides a simple and accurate method for detector efficiency calibration as has been described.⁷

2. Experimental Description

2.1 The Semi-fast Spill Beam

The present experiments were performed in the Enclosure 99 area of the Neutrino Target Hall at Fermilab. The beam available at this location was a resonantly extracted 400-GeV proton beam of approximately one millisecond duration. As can be seen in Fig. 1, the signal-to-noise ratio as observed with a beam current transformer of Fermilab design^{2,3} is good. However, the required gating time of ~ 2 msec did raise some problems. Secondary electrons from collisions between the beam-associated particles and matter, e.g., residual gas and vacuum pipe walls, in the

vicinity of the beam current transformer gap, could have sufficient time to pass through the gap and affect the transformer output signal. Studies of such effects are discussed in Section 3.4 below.

2.2 Beam Line

Relevant components along the beam line in the Enclosure 99 area are shown in Fig. 2. This area is located just downstream from six quadrupole magnets, which serve to shield it from beam halo. Two beam current transformers were used for all except the first irradiation. These were of the same design but one was read out by a voltage-to-frequency converter and the other by a charge integrator. The one with the charge integrator (denoted "new" in Fig. 2) could be calibrated at any time including during the proton pulse using a precision calibrator designed by one of the authors (C. Kerns). This integrator remained stable to within $\pm 0.1\%$ during the three month period when most of these measurements were made. The other transformer electronics also appeared to be stable during this period although it was calibrated only twice. The outputs of the two transformers, for a beam of $\sim 10^{13}$ protons per pulse differed by less than 1.5% throughout the three month period when most of these measurements were made. Three foil packets were irradiated one year later during further investigations of systematic effects. At that time the two toroid outputs differed by almost 5%; however, the mean cross section determined from their average differed by only 0.5% from the earlier measurements.

In addition to the two beam current transformers, the apparatus consisted of a vacuum chamber with remotely operated electric motors for

positioning targets plus special components for studying the possible effects of secondaries on the measurements: (1) a remotely-controlled "flag" for placing materials in the proton beam to produce secondaries; (2) an electromagnet for sweeping low-energy electrons out of the beam; (3) a vent for changing the air pressure at one beam current transformer relative to the other, (4) grids (not present in the early runs) for introducing electric fields in the beam pipe, and (5) insulators for electrically isolating various components.

2.3 Targets and Irradiations

Thirty-three irradiations of Cu targets were performed during the present experiment. With the exception of an initial exposure just downstream from the end window (Fig. 2), these irradiations were made in the vacuum chamber to eliminate corrections for secondary particles arising in that window. A variety of target configurations was used. The single or multiple foil stacks always had covers to compensate for or to measure ^{24}Na recoil losses from the center foil(s). Copper covers were normally used. In some cases Ti foils were placed upstream of the Cu stacks. Titanium is used at Fermilab as the end window material for beam pipes.

In normal practice, up to four target stacks were loaded into the vacuum chamber a day or two before a scheduled irradiation during periods of accelerator maintenance or development which provided convenient access to Enclosure 99. These were maintained in a withdrawn position 5 cm away from the beam. After suitable operating conditions had been established and performance of the current transformers checked, the targets were

irradiated sequentially using the electric motors to move the foils into and out of the beam line.

Typically, $4 - 20 \times 10^{14}$ protons were allowed to strike a target at an intensity of 10^{13} protons per pulse. Irradiations usually lasted 10 to 15 minutes. After each series, the targets were removed, autoradiographs were made, and circular samples (usually 3.2 cm in diameter centered on the beam spot) were punched out of the foils. Typical beam spots were circular or elliptical with a maximum diameter of ~ 2 cm along the major axis.

Of the total of 33 irradiated targets, foils from 28 were assayed at Fermilab, nine were assayed at Brookhaven National Laboratory (BNL) and eight at the European Organization for Nuclear Research (CERN). Shipments generally reached BNL and CERN less than two days after the end of the irradiation.

2.4 Assay of ^{24}Na

Although many γ -emitting nuclides are formed by the irradiation of Cu with high-energy protons,⁸ it can be seen in Table 1 that the resolution of a Ge(Li) spectrometer (~ 1.9 keV FWHM) is sufficiently high so that there are no major interferences with the assay of ^{24}Na . However, a low abundance γ ray from ^{55}Co is expected to make an $\sim 0.5\%$ contribution to the 1368.5-keV peak immediately after the end of an irradiation. While this relative contribution will grow with time, it reaches 1% only after 100 hours. Contributions of $\sim 0.5-1\%$ were also inferred from direct measurement of other ^{55}Co γ rays. The weak γ ray from ^{28}Mg will have an opposite effect. By raising the apparent valley between the lines of ^{24}Na

and ^{57}Ni it will result in an over subtraction of background from the 1368.5-keV peak. The net effect on our observed cross section will tend to cancel and not influence its use for beam monitoring purposes.

The ^{24}Na activities induced in the Cu foils were assayed at Fermilab by measuring the 1368-keV γ rays by Ge(Li) detectors placed with their cryostat entrance windows 10 cm from the center of the foils. These devices were calibrated frequently during the experiment with ^{60}Co sources from the National Bureau of Standards. Two detectors (active volume, $\sim 50\text{ cm}^3$) were used, each having a nominal efficiency 10% of that of a 7.6-cm diam by 7.6-cm thick NaI(Tl) detector. In mounting the standards and the ^{24}Na samples in plastic counting cards, micrometer measurements were made to correct for any deviations from 10 cm. The largest deviations resulted in a correction in efficiency of $\sim 1\%$. The 4096-channel γ -ray spectra were recorded at a gain of 0.5 keV/channel and stored on magnetic tape. These were subsequently analyzed to give the counting rates for the 1368-keV line of ^{24}Na and the 1332-keV line of ^{60}Co .

A variety of sources, in addition to ^{60}Co , was used to determine the efficiency of the Ge(Li) detector as a function of energy. These data defined the curve which was used to extrapolate the efficiency from 1332 keV to 1368 keV. Corrections for analyzer deadtime and pileup were made on the basis of 10-Hz pulses which had been introduced into the counting systems at their preamplifier inputs. No deviations of the decay of ^{24}Na from the expected 15.0-hr half life were observed.

Since the ^{60}Co standards were point sources, the ^{24}Na efficiencies derived from them are for point sources, also. Small corrections ($< 1\%$) for the actual extended ^{24}Na sources were made on the basis of the dependence of efficiency on lateral displacement observed for a ^{60}Co source combined with ^{24}Na distributions measured with a collimated β -particle detector.

Generally similar procedures for the assay of ^{24}Na were employed at BNL⁷ and CERN.⁹ One standard ^{60}Co source was counted at Fermilab, BNL, and CERN for intercomparison. The results agreed with previously determined efficiencies to $\pm 0.9\%$ (standard deviation for all three laboratories from the National Bureau of Standards value for the 1332-keV γ ray).

3. Analysis and Discussion

3.1 Calculation of Raw Cross Sections

From the 33 independent irradiations of single or multiple foil targets, a total of 48 assays of induced ^{24}Na activity were performed at the three participating laboratories. A cross section was calculated from each of these measurements using the disintegration rate and foil thickness measured at that particular laboratory in combination with the number of protons which passed through the foil as determined from the mean of the two toroid readings. Because the irradiations were short (< 30 min) compared to the ^{24}Na half life, no corrections were necessary for beam intensity fluctuations. The nominal error of each of these observed cross sections due to counting statistics only was the order of $\sim 0.5\%$.

3.2 Correction for Hadronic Secondary Effects

The raw cross sections will be somewhat higher than the true zero-target-thickness value because of ^{24}Na production by secondary hadrons born in a particular foil of a target or coming from other foils in the same stack or from sources such as vacuum windows or SEC's in proximity to that target. Because of the high threshold for ^{24}Na production from Cu, such effects should be small. Since our experiments were performed with a variety of Cu target thicknesses (43-373 mg/cm²), in some cases with additional Ti present on the upstream side, it was possible to verify this directly.

Energetic hadronic secondaries from the interaction of 400-GeV protons which are capable of producing ^{24}Na are expected to be forward peaked. The apparent cross section should then increase with the mass of material upstream of the foil center, since backstreaming particles have a negligible effect. Plotted in Fig. 3 as a function of this variable are the set of 28 cross sections observed at Fermilab. A trend beyond scatter is barely discernable for the points (open) based on all-Cu targets. Inclusion of data with added Ti (filled points) does show a small rise. A least squares fit to all the points gives the straight line,

$$\sigma = \sigma_0[1 + (7.3 \pm 1.5) \times 10^{-5}t] , \quad (1)$$

with a root-mean-square (rms) deviation of a single point from the line of 1.2%. For the limited range covered in the present work, a linear buildup of secondaries appears reasonable.

The small slope of Fig. 3 has several implications for future studies and practical applications. Time consuming vacuum accesses can be avoided because foils can be irradiated in air directly downstream of a standard Fermilab 5-mil (58 mg/cm^2) Ti end window with only an $\sim 0.4\%$ correction. Also, a typical Fermilab SEC (21 Ag-coated Al foils, each 1.7-mg/cm^2 thick and two 20-mg/cm^2 stainless steel end windows) will have only an 0.6% effect on a Cu monitor. This was verified in an auxiliary experiment where the influence of a SEC on a 134-mg/cm^2 Cu stack and vice versa were shown to be $<1\%$ in both directions.

Returning now to the analysis of the present data, Eq. 1 was used to extrapolate all individual measurements to zero target thickness. These were first averaged by laboratory and then overall giving the results shown in Table 2. The internal consistency is good, and, as can be seen in Fig. 4, the distribution of cross sections found run by run approximates that of a Gaussian.

3.3 Analysis of Errors

The width of the distribution in Fig. 4 is somewhat greater than the $0.5\text{-}1\%$ expected from counting statistics and the resolution of the 1368-keV γ line from the spectra. Some additional contribution to random errors may be due to foil thickness variations. Cross sections were calculated using the mean thickness of discs several times larger than the beam size. Detailed examination at CERN of foils used in this work showed that point-to-point variations never exceeded 2% from the mean. It is clear from Table 2 and Fig. 4 that the uncertainty on the mean cross

section due to these and any other random errors has been reduced to a very low value. The accuracy of the present experiment is determined by systematic errors.

One such error is the influence of the ^{55}Co and ^{28}Mg γ rays on the ^{24}Na assay which has been discussed above. Others might arise from systematic biases in the ^{24}Na - ^{60}Co comparison procedures used at all three laboratories or in the basic calibration of the ^{60}Co standards. Intercomparisons in the present work and those described by Cumming et al⁷ indicate it is unlikely that these could be as large as 1%.

We have not applied a correction for ^{24}Na production in the target foils outside of the punched circles. In most irradiations this amounted to ~0.3%. A major part of this appears to be due to irradiation by beam halo while the targets were in the retracted position. Although such halo is low (total $\sim 3 \times 10^{-5}$ of the protons in the beam pipe), foils were commonly in the retracted position for the order of a day. This hypothesis is supported by the increase in apparent out-of-beam ^{24}Na (up to ~1%) when thick materials were placed at the flag position (Fig. 2) to increase the halo, and by comparable levels of ^{24}Na in foils which were never inserted into the beam. We estimate the overall uncertainty due to all the above sources to be ~2%. Additional possible systematic errors in beam intensity measurements are given special attention below.

3.4 Uncertainties in Proton Flux measurements

A number of auxiliary experiments were performed in which operating conditions in the Enclosure 99 area were intentionally perturbed from normal to reveal or enhance possible systematic effects. Although a beam current transformer can be calibrated absolutely in terms of known

electrical standards, it cannot distinguish between primary beam protons and secondary charged particles which may pass through its aperture during the time its electronic gate is open. Secondary electrons may result from collisions of the proton beam with the residual gas in the beam pipe (pressure ~30 mtorr) or from surface emission as the protons strike the vacuum pipe walls or the target itself. For 1-msec spills, these electrons have time to move significant distances under the influence of small electric fields.

We observed that thin metallic foils which were electrically connected to the same ground potential as the beam pipe could affect the proton flux measurements made by a beam current transformer several meters up- or downstream from that foil. We do not believe that an individual ejected secondary electron traveled all the way from the foil to the gap of the transformer because the magnet placed between the two (Fig. 2) to sweep out these electrons had no effect. Rather, we think a potential difference resulting from electrons replacing the leaving secondaries caused electrons local to the transformer to move through the transformer gap. The change was at most 3% and the direction of the effect (\pm) depended on the direction of the electrons relative to the proton beam. Isolating the foils from ground so that they charged up to their equilibrium potential eliminated this problem.

Intentionally introducing a potential on a grid in the beam path could induce enough electrons to cross the gap of the current transformer to radically change its response to a given proton beam. This effect could also be produced by applying a potential to a conductor inside the

beam pipe which the proton beam did not strike. This change was not due to an electrostatic effect on the current transformer because its calibration remained constant, independent of the potential applied. Examination of the transformer output showed a large negative overshoot shortly after passage of the proton beam, which we interpret as due to flow of electrons towards the positive electrode. Isolating the beam pipe in the region around the current transformer with thin insulating windows (13 mg/cm^2 Kapton[®] plastic) interrupted this flow and rendered the transformer response independent of such potentials. Several attempts were made to search for potential differences present under normal operating conditions. No evidence was found; however, an exhaustive study was not carried out.

The effect of residual gas in the vacuum pipe was also studied. Increasing the pressure above its base value of 30 mtorr increased the output of the beam current transformer by 2% per 100 mtorr if the electronic gate (see Fig. 1) was open for 17 msec but resulted in negligible increase if the gate was open for the standard ~ 2 msec. This indicated passage of relatively slow-moving electrons through the transformer gap opposite to the beam direction.

Placing thick (up to 460 mg/cm^2 Ti) foils one meter upstream (the flag location, Fig. 2) caused an increase in the downstream transformer output. That such an increase is indeed due to interactions in the foil and not to intercepting an electron component of the beam is shown by the fact that this increase was proportional to the Ti thickness. The percentage increase was approximately the same as the

percentage of extra halo, due to extra secondaries from the foil, striking the core of the transformer. Under normal conditions, when the halo was 3×10^{-5} , the effect was negligible.

We conservatively assign a 2% systematic uncertainty to the beam monitoring procedure. This is based on the possibility that secondary electrons traveling with the beam or moving in response to potentials set up by the beam could affect the current transformer readings. It should be noted that future experiments utilizing single-turn or single-bunch extraction would be extremely valuable in confirming this, for the width of the transformer gate could be reduced by a factor of 100 or more.

3.5 Results

The cross section for the production of ^{24}Na from Cu by 400-GeV protons determined in the present experiment is 3.90 ± 0.11 mb. The error on this value represents the combination of the systematic errors discussed above with the negligibly small random error on our measurements (see Table 2). The energy dependence of this and other beam monitor reactions is indicated in Table 3. Independent absolute cross sections at both energies have been measured only for the $^{12}\text{C}(p,pn)^{11}\text{C}$ reaction^{10,11}. The $^{63,65}\text{Cu}(p,x)^{24}\text{Na}$ reaction at 28 GeV was determined relative to the $^{27}\text{Al}(p,3pn)^{24}\text{Na}$ cross section, while the $^{27}\text{Al}(p,3pn)^{24}\text{Na}$ cross section at 300 GeV is relative¹² to the $^{12}\text{C}(p,pn)^{11}\text{C}$ value.

The $9.6 \pm 4.2\%$ increase in the $^{63,65}\text{Cu}(p,x)^{24}\text{Na}$ cross section between 28 and 400 GeV was somewhat unexpected as total reaction cross sections are essentially independent of energy in this region.¹³ Some

early studies¹⁴ of ^{24}Na production from V and Co targets had also suggested energy independence. However, that conclusion was based on an assumed energy invariance of the $^{27}\text{Al}(p,3pn)^{24}\text{Na}$ cross section. As can be seen in Table 3, that monitor reaction is poorly known at 300 GeV. The rise may be some evidence that ^{24}Na production from Cu is like ^{24}Na production from heavier elements such as Au, where an ~ 10% rise in cross section is observed,¹⁵ rather than like the simpler $^{27}\text{Al}(p,3pn)^{24}\text{Na}$ and $^{12}\text{C}(p,pn)^{11}\text{C}$ reactions.

4. Conclusions

The accurate cross section provided by the present experiment for the $^{63,65}\text{Cu}(p,x)^{24}\text{Na}$ reaction at 400 GeV and the detailed studies of secondary and possible systematic effects serve to establish this reaction as a benchmark for further foil activation studies and practical applications for beam monitoring at high energies. The reaction is currently used to calibrate secondary emission chambers for monitoring high intensity proton beams at Fermilab and CERN. The collaboration between Fermilab, BNL and CERN has resulted in an intercomparison which should be beneficial to other high energy physics experiments.

Acknowledgments

The authors are grateful to A. L. Read, L. Coulson, D. Jovanovic, and R. Stefanski of Fermilab, L. W. Smith of BNL, and G. Munday, K. Goebel, C. Bovet, and R. Billinge of CERN for their continued support and encouragement. J. Baldwin was responsible for the ^{24}Na assay at Fermilab, and A. Regelbrugge at CERN. J. Smalley (deceased) assisted in assembling the apparatus and with data processing. B. Ewing assisted in the

preparation of the BNL target chamber and foil drives. Finally the experiment would not have been possible without the enthusiastic support of the Neutrino Department, Accelerator Division, and others at Fermilab where the experiment was performed. This research was supported in part by the U.S. Department of Energy.

References

1. V. Agoritsas and R.L. Witkover, IEEE Trans. Nucl. Sci. NS-26, No. 3, 3355 (1979).
2. C.R. Kerns, IEEE Trans. Nucl. Sci. NS-20, No. 1, 204 (1973).
3. C.R. Kerns, IEEE Trans. Nucl. Sci. NS-22, No. 3, 1104 (1975).
4. R.G. Korteling and A.A. Caretto, J. Inorg. Nucl. Chem. 29, 2863 (1977).
5. J.B. Cumming, Ann. Rev. Nucl. Sci. 13, 261 (1963).
6. E.P. Steinberg, A.F. Stehney, C. Stearns, and I. Spaletto, Nucl. Phys. A113, 265 (1968).
7. J.B. Cumming, V. Agoritsas, and R. Witkover, Nucl. Instrum. Meth. 180, 37 (1981).
8. J.B. Cumming, R.W. Stoenner, and P.E. Haustein, Phys. Rev. C14, 1554 (1976).
9. A. Chapman-Hatchett, G. Cultrut, J. Dieperink, A. Fasso, W. Kalbreier, A. Muller, S. Peraive, M. Nielsen, A. Regelbrugge, G. R. Stevenson, and D. Thomas, CERN Report SPS/AB7/Int. 79-1 (1979).
10. J. B. Cumming, G. Friedlander, and S. Katcoff, Phys. Rev. 127, 950 (1962).
11. S.B. Kaufman, M.W. Weisfield, B.D. Wilkins, D. Henderson, and E.P. Steinberg, Phys. Rev. C13 253 (1976).
12. S. B. Kaufman as quoted in ref. 15.
13. A.S. Carroll, I-H. Chiang, T.F. Kycia, K.K. Li, M.D. Marx, D.C. Rahm, W.F. Baker, D.P. Earty, G. Giacomelli, A.M. Jonckheere, P.F.M. Koehler, P.O. Mazur, R. Rubinstein, and O. Fackler, Phys. Lett. 80B, 319 (1979).

14. S. Katcoff, S.B. Kaufman, E.P. Steinberg, M.W. Weisfield, and B.D. Wilkins, Phys. Rev. Lett. 30, 1221 (1973).
15. S.B. Kaufman, M.W. Weisfield, E.P. Steinberg, B.D. Wilkins, and D. Henderson, Phys. Rev. C 14, 1121 (1976).

Table 1. Decay properties and cross sections of isotopes possibly interfering with ^{24}Na assay in Cu by γ -ray spectroscopy.

Product	Half Life (hr)	E_γ (keV)	I_γ (%)	σ (mb) ^a	A_γ^0 (rel)
^{56}Co	1891	1360.2	4.29	4.3	0.04
^{24}Na	15.0	1368.5	100	3.9	100
^{55}Co	17.5	1370.0	3.0	0.81	0.53
^{28}Mg	21.1	1372.8	4.7	0.42	0.36
^{57}Ni	36.1	1377.6	77.9	0.46	3.8

^aFrom ref. 8 and the present work.

Table 2. Cross sections extrapolated to zero target thickness for the
 $^{63,65}\text{Cu}(p,x)^{24}\text{Na}$ reaction at 400 GeV.

Laboratory	Number of Measurements	Mean Cross Section (mb) ^a	Standard Deviation of a Point (%)
Fermilab	28	3.92 ± 0.01	1.2
BNL	9	3.90 ± 0.02	1.5
CERN	8	3.87 ± 0.03	2.5
All	45	3.90 ± 0.01	1.6

^aStandard errors of the means include random effects only.

Table 3. Energy dependence of selected monitor reaction cross sections.

Reaction	Cross Section (mb)		
	28 GeV	300-400 GeV	Ratio
$^{63,65}\text{Cu}(p,x)^{24}\text{Na}$	3.56 ± 0.09^a	3.90 ± 0.11^b	1.096 ± 0.042
$^{27}\text{Al}(p,3pn)^{24}\text{Na}$	7.92 ± 0.18^c	8.1 ± 0.6^d	1.022 ± 0.079
$^{12}\text{C}(p,pn)^{11}\text{C}$	25.9 ± 1.2^e	24.6 ± 1.6^f	0.950 ± 0.076

^aRef. 8, corrected for a revised $^{27}\text{Al}(p,3pn)^{24}\text{Na}$ cross section (ref. 7).

^bPresent work.

^cRef. 7.

^dRef. 12.

^eRef. 10.

^fRef. 11.

Figure Captions

- Fig. 1. Oscilloscope trace of the beam current transformer output superimposed on the electronic gate of the charge integrator. Oscilloscope settings: 0.1 V/div. vertical, 0.2 msec/div. horizontal.
- Fig. 2. Components along the beam line in the Enclosure 99 area of Fermilab.
- Fig. 3. Dependence of the apparent cross section for the $^{63,65}\text{Cu}(p,x)^{24}\text{Na}$ reaction at 400 GeV on the mass of material upstream of the center of the particular foil examined. Open points are for all-Cu targets, filled ones for cases where Ti was present on the upstream side. The straight line is a least squares fit to the points. A few error flags indicate the 1.2% root-mean-square deviation of points from that line.
- Fig. 4. Distribution of $^{63,65}\text{Cu}(p,x)^{24}\text{Na}$ cross sections observed at the three participating laboratories as indicated. The position of the mean is shown with an arrow. The curve is a Gaussian with the same mean and standard deviation as the histogram.

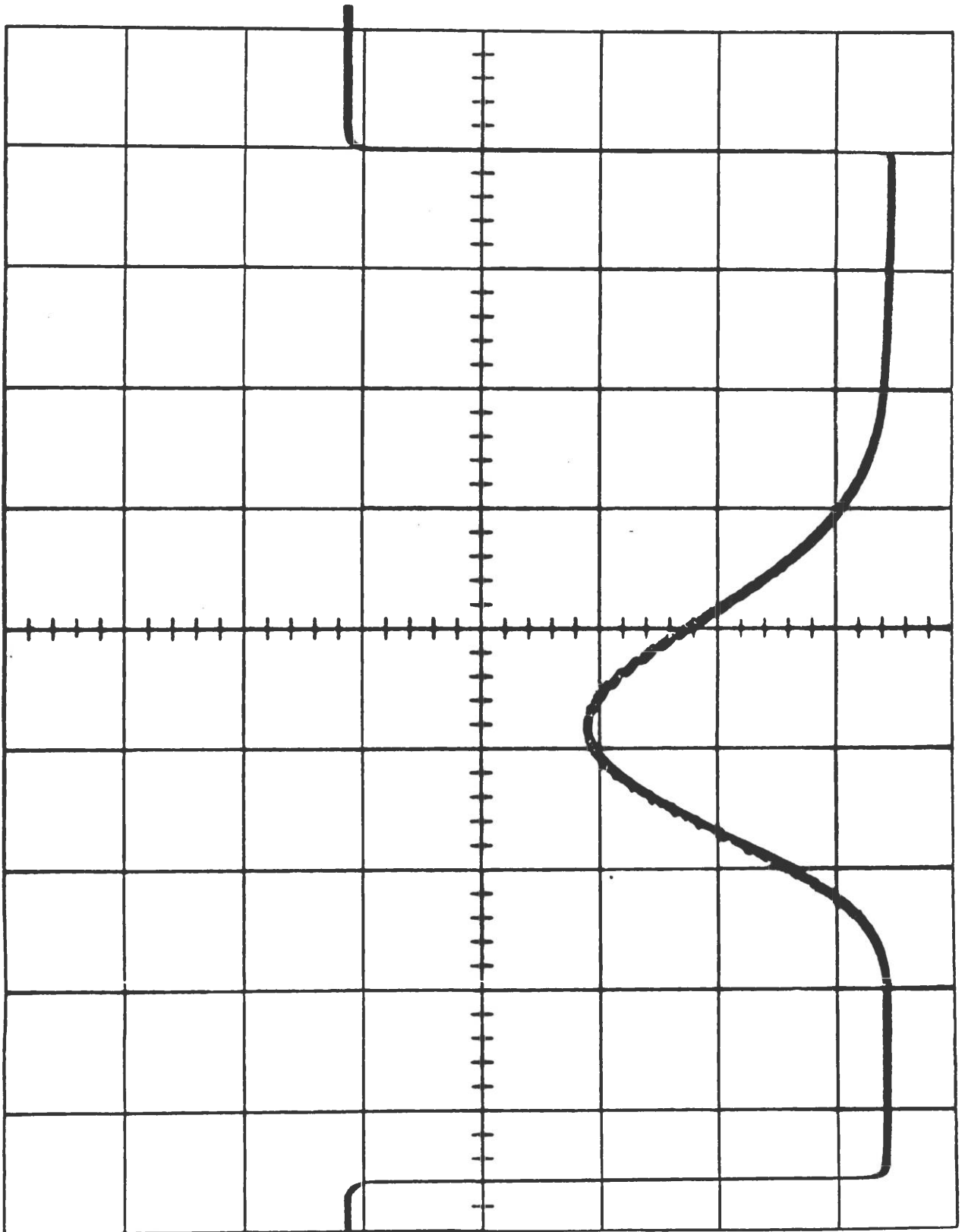


Fig. 1

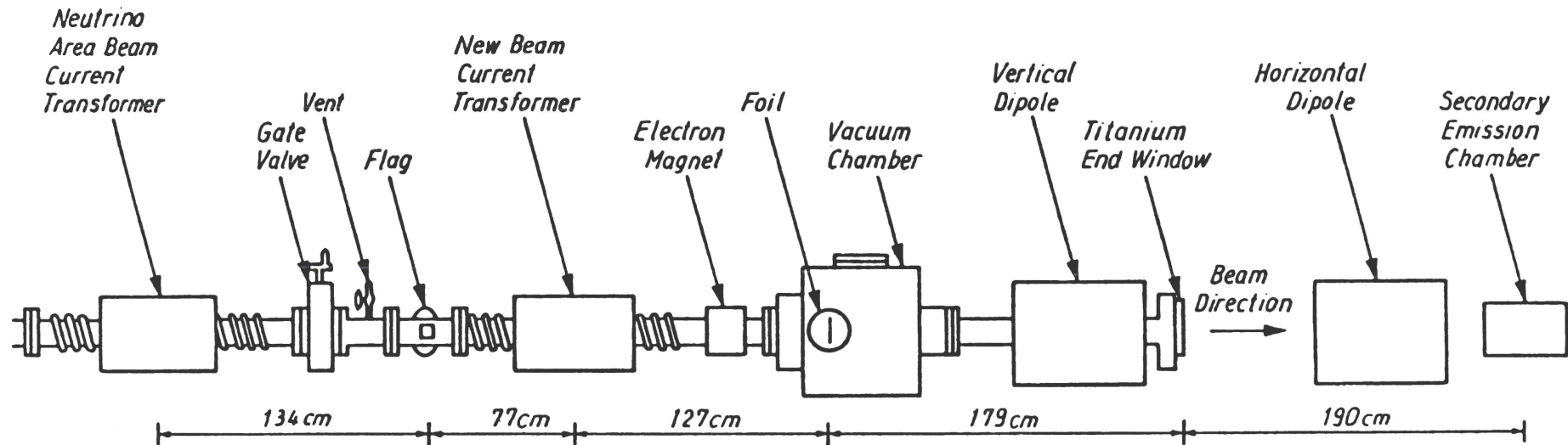


Fig. 2

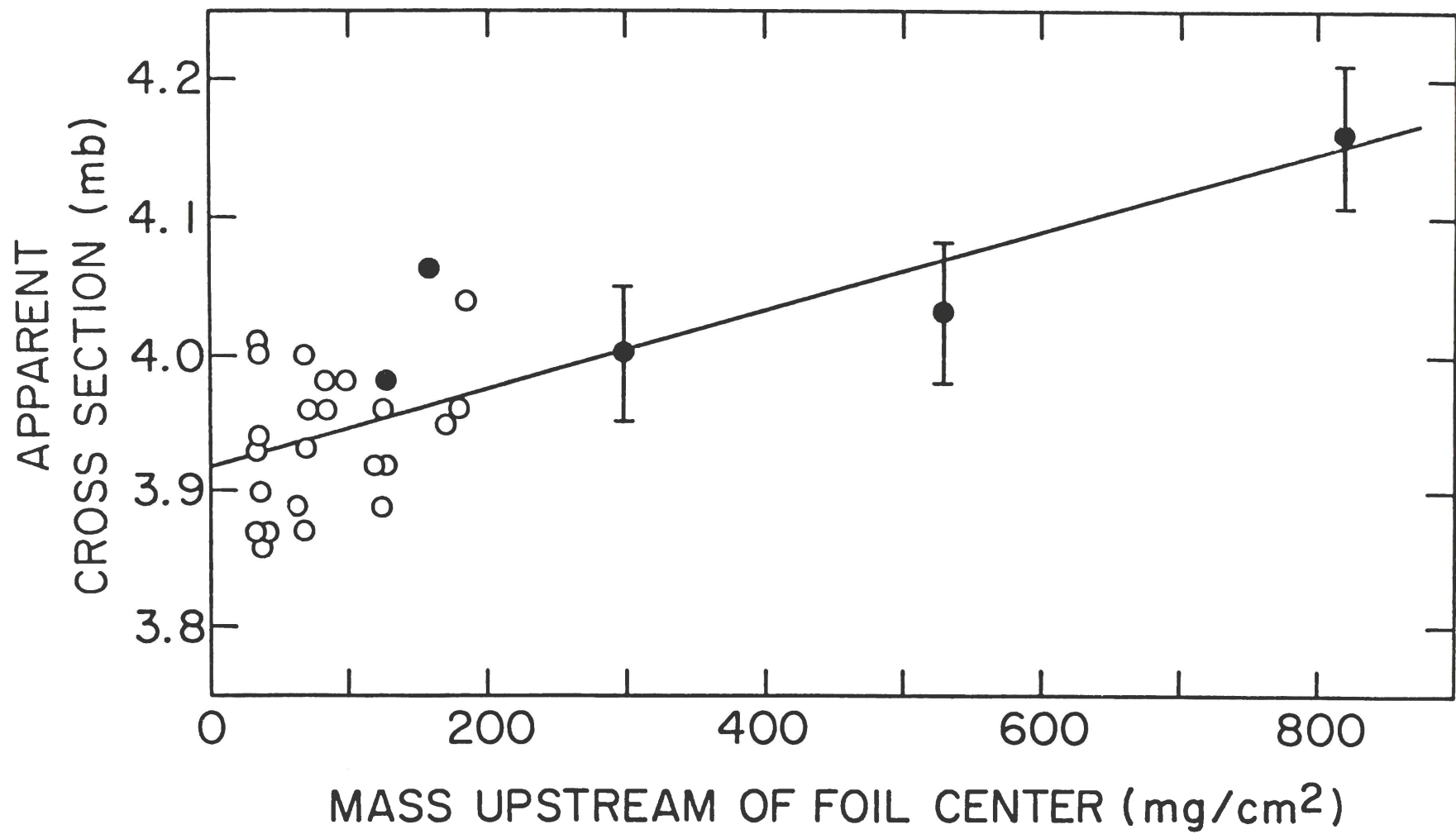


Fig. 3

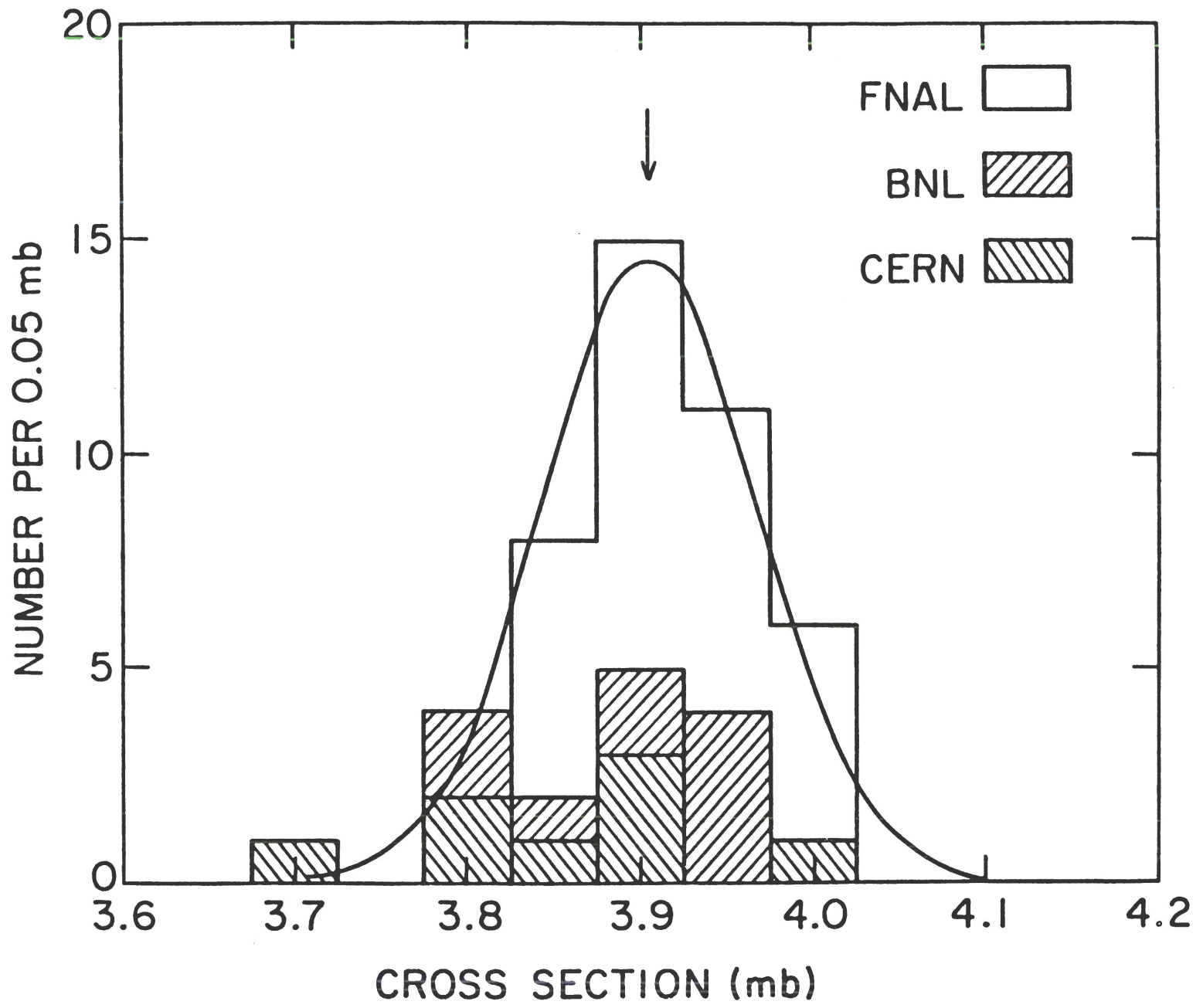


Fig. 4